Chinese Science Bulletin

Rupture of the 2004 Sumatra-Andaman earthquake inferred from direct P-wave imaging

LIU Ning[1†], CHEN QiFu[1], NIU FengLin[1,2] & CHEN Yong[1]

[1] Institute of Earthquake Science, China Earthquake Administration, Beijing 100036, China;
[2] Department of Earth Sciences, Rice University, Houston, TX 77005, USA

The Sumatra-Andaman earthquake on December 26, 2004 is the first well recorded gigantic earthquake (moment magnitude M_W 9.3) by modern broadband seismic and Global Positioning System networks. The rich seismic and geodetic recordings have documented unprecedented details about the earthquake rupture, coseismic and postseismic deformations. This is a report of detailed images of the rupture process using the first-arriving compressional waves recorded by the China National Digital Seismic Network (CNDSN). An improved imaging condition was employed to account for the sparse distribution of the CNDSN stations. The resulting images are consistent with the major rupture features reported by previous seismic and geodetic studies. It is found that the earthquake rupture initiated at offshore of northwestern Sumatra and propagated in the north northwest direction at a speed of 2.7 ± 0.2 km/s. The rupture continued for at least 420 s and extended about 1200—1300 km along the Andaman trough with two bursts of seismic energy.

direct imaging, earthquake rupture, Sumatra-Andaman earthquake, CNDSN

The Sumatra-Andaman earthquake with a moment magnitude of 9.3[1,2] occurring on 26 December 2004 is the first gigantic earthquake that is well recorded by modern broadband seismic and Global Positioning System (GPS) networks[2,3]. The rich seismic and geodetic recordings have been extensively analyzed to understand details about the earthquake rupture, coseismic and postseismic deformations. While the Global Seismic Network (GSN) played a significant role in determining the source location, mechanism and rupture propagation[1,2,4—7], dense regional networks at teleseismic distance, for example, the High sensitive short-period Network (Hi-Net) in Japan[8] and the German Broadband Region Seismic Network (GRSN)[9] also exhibited their importance in imaging the rupture process. Here we demonstrate that the newly built China National Digital Seismic Network (CNDSN), despite of being sparse, can play an equivalently important role in deciphering earthquake rupture processes with a specifically designed imaging condition.

1 Data and methodology

CNDSN consists of 48 real-time transmission broadband seismic stations at 500—600 km spacing (Figure 1(a)). The stations are equipped with three types of broadband sensors, STS-2, JCZ-1 and CTS-1. They have a flat response in the frequency bands of 120 s—40 Hz, 360 s—50 Hz and 120 s—50 Hz, respectively. The CNDSN stations are located at about 20°—55° away from epicenter of the great Sumatra-Andaman earthquake with azimuths ranging from –25° to 43° (Figure 1(b)). Although station spacing is apparently larger, our seismic network covers a wider azimuth range than those of both Hi-Net and GRSN.

To avoid waveform triplications associated with the upper mantle discontinuities, we selected 29 stations

Received November 10, 2006; accepted May 8, 2007
doi: 10.1007/s11434-007-0286-x
†Corresponding author (email: bjlemon@163.com)
Supported by National Key Technologies R&D Program of China (Grant No. 2005DIA3J117)

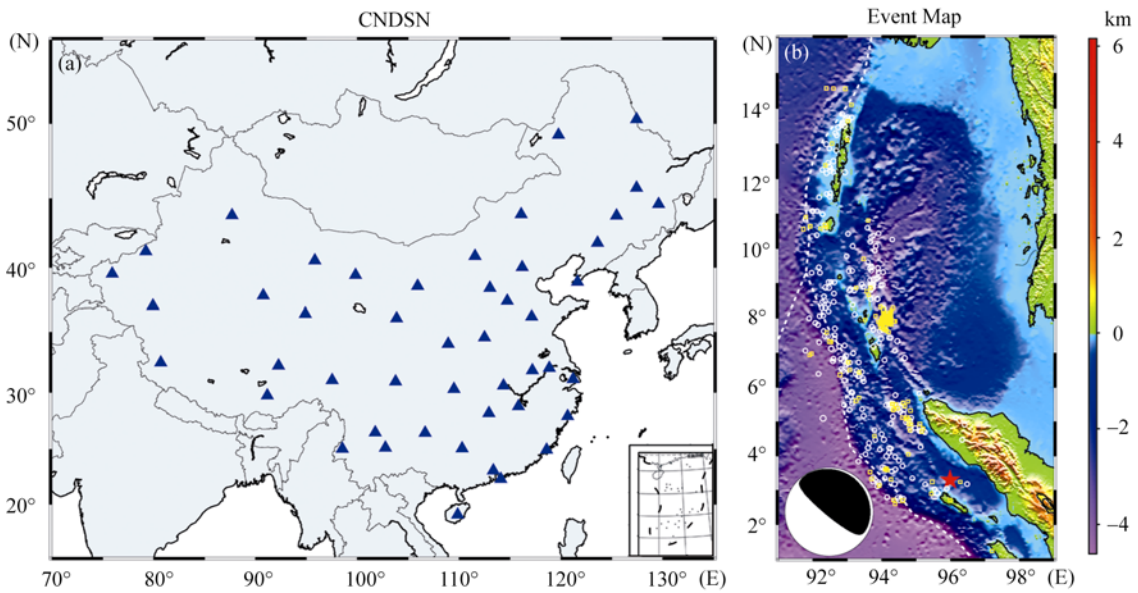

Figure 1 (a) Distribution of 48 stations (solid blue triangles) of the CNDSN; (b) source region of the 26 December 2004 Sumatra-Andaman earthquake. The epicenter and Harvard CMT solution are shown by red star and beach ball. Aftershocks occurring from 26 December, 2004 to 31 January, 2005 are shown by white dots. White dashed line indicates the NUVEL1 plate boundary.

with an epicentral distance greater than 30° to perform the direct imaging analysis of the earthquake rupture. 27 of the 29 seismograms are shown in Figure 2 (the left two are not shown simply to avoid waveform overlaps). It should be noted that the first 60-s waveforms exhibit remarkable similarity across the entire array.

Following Ishii et al.[8], we employed a back-projection method to image the progression of the transient rupture front. It is a simplification of wavefield reverse-time migration, a tool for imaging structure in reflection seismology. The migration is based on the equivalence of the source and receiver in the wave propagation equation. Each station can be considered a source and the seismic rays radiated from them merge at the epicenter. In so doing, we first assumed that the rupture front propagated horizontally at depth of 30 km. We divided the source region between 91°E to 99°E and 16°N to 30°N (Figure 1(b)) into a set of grids with an interval of 0.2°. These grids are considered as potential transient sources where seismic energy was radiated at different time[10].

For the jth source location, the seismograms are summed to make the stack s_j during the time window ($t_n - T_0/2 - t_n + T_0/2$):

$$s_j(t_n) = \sum_{t=t_n-T_0/2}^{t_n+T_0/2} \left(\sum_{k=1}^{M} U_k(t - t_{jk}^p + \Delta t_k)/A_k \right)^2. \quad (1)$$

Furthermore, the semblance of seismograms S_j:

$$S_j(t_n) = \frac{\sum_{t=t_n-T_0/2}^{t_n+T_0/2} \left(\sum_{k=1}^{M} U_k(t - t_{jk}^p + \Delta t_k)/A_k \right)^2}{M \sum_{t=t_n-T_0/2}^{t_n+T_0/2} \sum_{k=1}^{M} U_k^2(t - t_{jk}^p + \Delta t_k)/A_k^2}, \quad (2)$$

where $U_k(t)$ is the vertical-component seismogram recorded at the kth station, M the station numbers, and t_{jk}^p the theoretical P-wave travel time from the jth source to the kth station based on IASP91 model[11]. Δt_k denotes timing corrections obtained from waveform cross correlation of the first-arriving P waves. The correction enhances the coherence of waveforms by taking account of the diversity of ray paths. A_k is the peak amplitude of the seismogram. Semblance S_j in formula (2) and linear stack s_j can be considered as the probability of the grid point as a transient source and the energy radiated from it. The maximum semblance is shown as function of time in Figure 2(c) (solid line). For comparison, semblance calculated at the initial point of the rupture is shown by dashed line. We found that the weighted stack $E_j(t_n) = s_j(t_n) \cdot S_j(t_n)$ is more efficient in focusing the rupture front image (Figure 2(c)).

2 Analyses

Since the S wave arrives at the CNDSN station within about 400 s after the direct P wave, we used only the

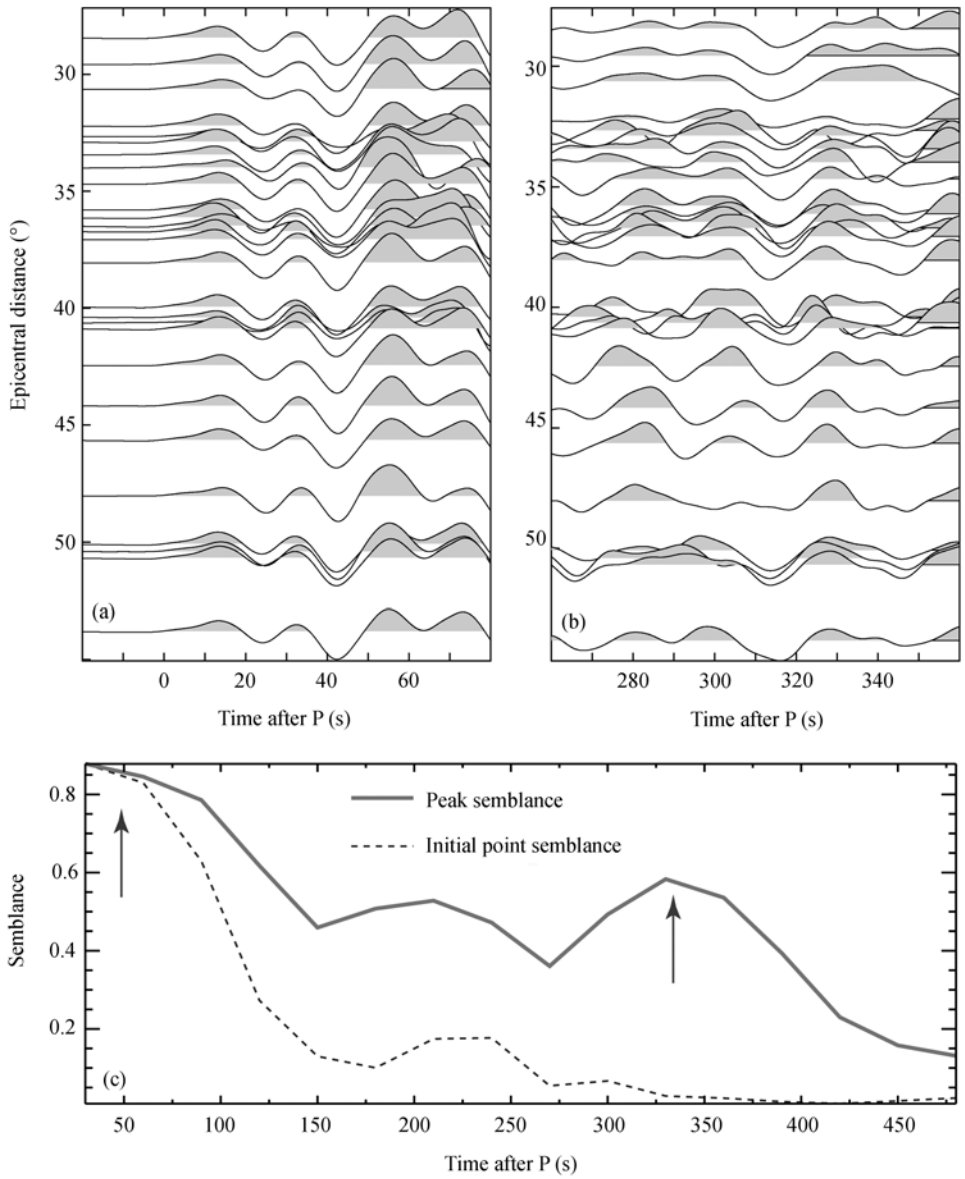

Figure 2 Selected seismic record, especially the corresponding seismic waveforms in the first (a) and second (b) impulse time windows (10—100s Butterworth filter is applied). So there is a high semblance value by rearranging and later filtering the waveform while taking peak semblance point as transient source. (c) The peak semblance of seismogram calculated from different grids in source region in consecutive time windows is given by solid line, and for comparison, the semblance resulting from the initial point of rupture is shown by dashed line. Arrows represent the peak semblance value corresponding to the first and second impulse.

first 7 min of the waveforms to perform direct imaging. Before the imaging we performed a few steps of data preprocessing. We first removed the instrument responses from the velocity records, and then converted the velocity records to the displacement seismograms. However, no filtering was involved in this processing. Thus the different responses of the three types of sensor are expected to have no effect on our results. Figure 3 shows the maxima of seismic energy obtained for each 1 minute time frame. It is evident that seismic radiation has a broad elongated peak in the northeast direction. The peak radiations in our images are broader than those obtained by Ishii et al.[8], but are much more focused than those imaged by Krüger et al.[9], which has a peak size of ~20° by 20°. The broad peaks may reflect the true feature of the rupture. But it is more likely caused by the large station spacing of the CNDSN and also the source-receiver geometry. The CNDSN stations are located in the northwest direction of the earthquake, which leads to a relatively poor resolution in the northeast di-

rection. In term of both the station spacing and source-receiver geometry, CNDSN is very similar to GRSN. This explains why we also obtained northeast oriented broad peaks in our images. As we employed a weighted stack algorithm in our imaging, we were able to make the wave front more focused. On the other hand, the Hi-Net has a station spacing of 20 km and consists of about 700 short-period stations, and it is not difficult to understand why the Hi-Net images are sharper than ours.

Here are a few major features summarized from Figure 3. Relatively large seismic energy was released in the first 90 s (0—60s and 30—90s in Figure 3), during this time interval the wave front moved very little. This indicates that Sumatra-Andaman earthquake initiated slowly for the first 40 to 60 s, consistent with what was found by Ammon et al.[5]. The rupture front, indicated by the position of the peak energy radiation, then moved steadily toward the north northwest direction at a speed of 2.7±0.2 km/s (Figure 4(a)), and continued for at least 420 s.

The amount of released seismic energy also appears to vary with time. We saw two very low release periods in two time intervals at 120—180 s and 240—300 s after the first arrival, and two high energy bursts in 30—90 s and 300—360 s time windows. This observation is consistent with the results of Ishii et al.[8] and Krüger et al.[9]. Ammon found a third burst in a later time window of 450—500 s[5], which is impossible for us to confirm because we can image only the first 7 min of the rupture. The geographic distribution of the total amount of seismic energy radiated in the first 7 min is shown in Figure 4(b). We found the two large energy bursts are also geographically separated. The second one is located around 9.3°N and 92.7°E, about 750 km away from the first one. This also agrees well with those found by Ishii et al.[8] and Krüger et al.[9]

The 26 December, 2004 Sumatra-Andaman earthquake occurred on the interface of Indo-Australian plate and Burma microplate. The fault released strains that had been accumulated for centuries from ongoing subduction of the India plate along Sunda trench and beneath the Burma microplate[12—14], accompanied by upheaval of benthal. Compared with the settings of previous earthquakes, the distinctive features of this great earthquake are that the dip, age of the subducting plate and gradient in obliquity of interplate motion increase toward the north-northwest between Sumatra and the Andaman Islands[2]. All of these setting characteristics may lead to descending of plate coupling. Our results indicate that there are at least three stages in rupture process. In the first stage the rupture propagated slowly, where the fault was well-coupled in the south (Figure 3, 0—120 s). Large seismic energy was release during this stage. As the rupture propagates toward the north at the northern end of the Sumatra Island, the rupture enters into the second aseismic stage (Figure 3, 120—300 s). It is likely that most of the released energy was used for the continuation of the rupture. In the third stage the rupture appears to be rejuvenated and featured by high seismic energy release with a high propagation velocity (Figure 3, 300—420 s). This is probably related to the very weak coupling in the northern end of the subduction.

Our analysis indicates that the 2004 Sumatra-Andaman great earthquake rupture lasted for at least 420 s. The long source time function of this earthquake has been recognized by all the previous studies[4,8,9], and is probably the trade mark of this earthquake. It is definitely the longest one recorded. Yet it is also universally recognized that the rupture extended about 1200—1300 km which can be also confirmed from the distributions of aftershocks (Figure 4(b))[1,2,4,5,7,8]. Also cumulative radiated energy in Figure 4(b) agrees very well with coseismic slip inverted from geodetic data by of Subarya et al.[15]. The geodetic data used in their inversion include the near-field GPS observation, uplift and subsidence measurements of coral reef obtained from field study and remote sensing images.

3 Conclusions

We applied a direct imaging technique to the P waves recorded at the CNDSN stations generated by the 2004 great Sumatra-Andaman earthquake. The CNDSN images are used to understand the earthquake rupture processes. Throughout this study we have reached the following conclusions:

(1) Our study demonstrates that it is feasible to use the CNDSN station as a large seismic array for imaging the rupture process of 2004 Sumatra-Andaman earthquake. Our results are consistent with previous analyses using data recorded by global and regional, seismic and GPS networks.

(2) We have proposed an imaging scheme for seismic networks with sparse station distribution. By using a

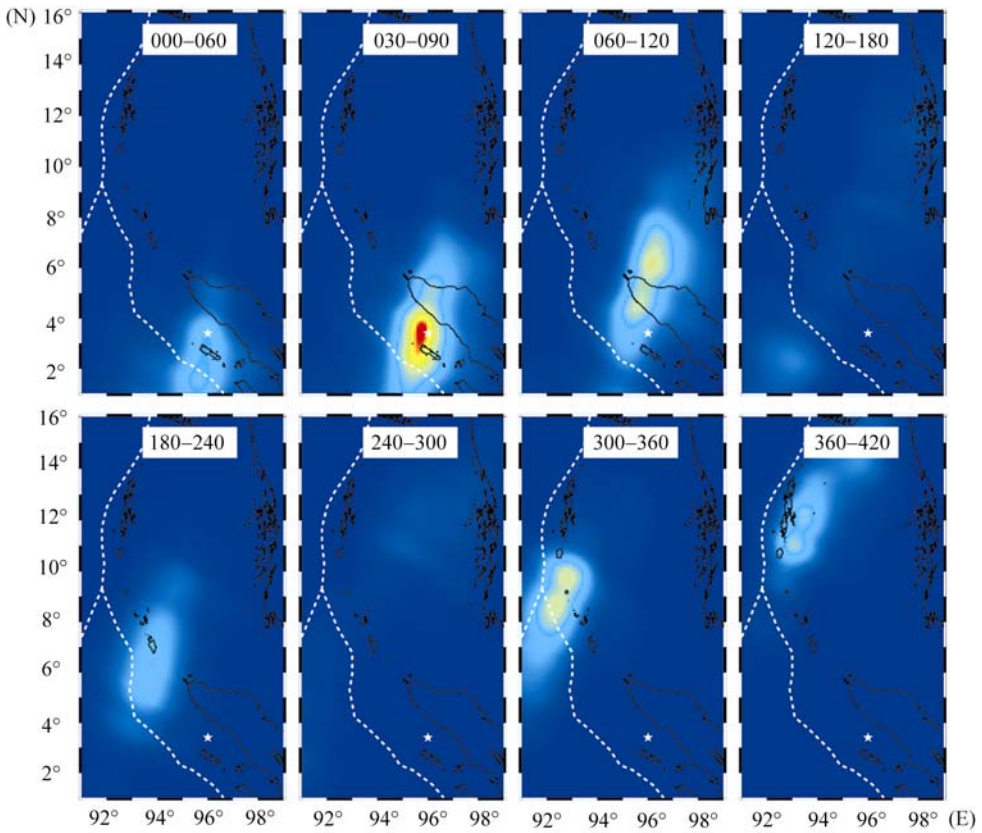

Figure 3 Distribution of energy radiation in consecutive 60-s intervals. The epicenter provided by NEIC is indicated by a white star.

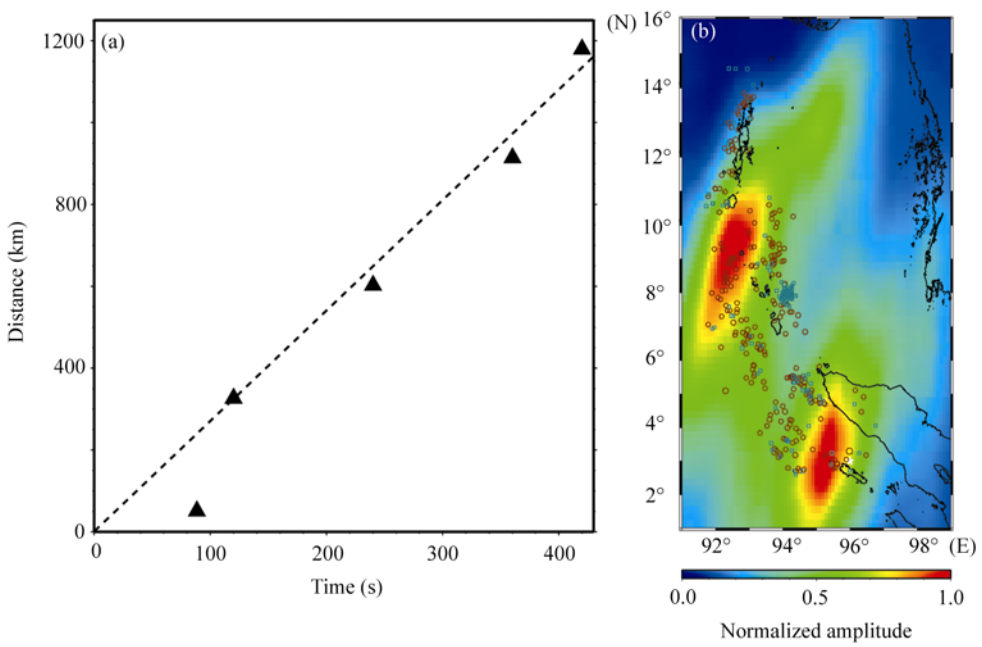

Figure 4 (a) Rupture distance along the fault versus time. The solid triangle is the location of peak energy radiation in the 30—90 s, 60—120 s, 180—240 s, 300—360 s and 360—420 s time windows. The dashed line is the L2-norm linear regression of the last four points. The slope gives an average rupture speed of 2.7 km/s. Notice that the first triangle is far below the dashed line, indicating that the propagation speed is low for the first part of rupture. (b) Distributions of aftershock occurring from 26 December, 2004 to 31 January, 2005 and cumulative radiated energy.

weighted stacking algorithm, we were able to obtain focused images of the rupture fronts of the Sumatra-Andaman earthquake with the CNDSN recordings, leading to robust estimates of rupture direction, velocity and duration.

(3) Our method requires no input on fault geometry which is usually estimated from aftershock distribution. Thus it provides a rapid determination of duration, direction and rupture length of large earthquakes. These observations are key parameters for rapid assessment of immediate seismic hazard.

The authors thank China Earthquake Networks Center (CENC) for providing us the seismic data.

1 Stein S, Okal E. Speed and size of the Sumatra earthquake. Nature, 2005, 434: 581－582 [DOI]

2 Lay T, Kanamori H, Ammon C, et al. The great Sumatra-Andaman earthquake of 26 December 2004. Science, 2005, 308: 1127－1133 [DOI]

3 Wang M, Zhang P Z, Shen Z K, et al., Far-field coseismic displacements associated with the great Sumatra earthquake of December 26, 20004 and March 29, 2005 constrained by Global Positioning. Chin Sci Bull, 2006, 51(14): 1771－1775

4 Ni S, Kanamori H, Helmberger D. Seismology - Energy radiation from the Sumatra earthquake. Nature, 2005, 434: 582－582[DOI]

5 Ammon C, Ji C, Thio H, et al. Rupture process of the 2004 Sumatra-Andaman earthquake. Science, 2005, 308: 1133－1139[DOI]

6 Park J, Song T, Tromp J, et al. Earth's Free Oscillations Excited by the 26 December 2004 Sumatra-Andaman Earthquake. Science, 2005, 308: 1139－1144[DOI]

7 Tsai V C, Nettles M, Ekström G, et al. Multiple CMT source analysis of the 2004 Sumatra earthquake. Geophys Res Lett, 2005, 32, L17304, doi:10.1029/2005GL023813

8 Ishii M, Shearer P M, Houston H, et al. Extent, duration and speed of the 2004 Sumatra-Andaman earthquake imaged by the Hi-Net array. Nature, 2005, 435: 933－936

9 Krüger F, Ohrnberger M. Tracking the rupture of the Mw = 9.3 Sumatra earthquake over 1150 km at teleseismic distance. Nature, 2005, 435: 937－939

10 Spudich P, Cranswick E. Direct observation of rupture propagation during the Imperial Valley earthquake using a short baseline accelerometer array. Bull Seismol Soc Am, 1984, 74: 2083－2114

11 Kennett, B L N, Engdahl E R. Traveltimes for global earthquake location and phase identification, Geophys J Int, 1991, 105: 429－465 [DOI]

12 Fitch T J. Plate Convergence, Transcurrent Faults, and Internal Deformation Adjacent to Southeast Asia and the Western Pacific. J Geophys Res, 1972, 77(23): 4432－4460

13 Sieh K, Natawidjaja D H. Neotectonics of the Sumatran fault, Indonesia. J Geophys Res, 2000, 105(28): 295-326

14 Sieh K, Natawidjaja D H, Chlieh M, et al. The giant subduction earthquakes of 1797 and 1833, West Sumatra: Characteristic couplets, uncharacteristic slip. Eos Trans AGU, Fall Meet Suppl, Abstract, 2004. 85: T12B-04 [DOI]

15 Subarya C, Chlieh M, Prawirodirdjo L, et al. Plate-boundary deformation associated with the great Sumatra–Andaman earthquake. Nature, 2006, 440: 46－51[DOI]